JCTC Journal of Chemical Theory and Computation

Molecular Dynamics Simulation of Iminosugar Inhibitor−Glycosidase Complex: Insight into the Binding Mechanism of 1-Deoxynojirimycin and Isofagomine toward β-Glucosidase

Jin-Ming Zhou,*,† Jun-Hong Zhou,‡ Yi Meng,† and Min-Bo Chen*,†

Department of Computer Chemistry and Cheminformatics, Shanghai Institute of Organic Chemistry, Chinese Academy of Sciences, 354 Fenglin Lu, 200032, Shanghai, China, and Chemical and Pharmaceutical Institute, East China University of Science and Technology, 130 Meilong Lu, 200237, Shanghai, China

Received July 11, 2005

Abstract: The binding mechanism of iminosugar inhibitor 1-deoxynojirimycin and isofagomine toward β-glucosidase was studied with nanosecond time scale molecular dynamics. Four different systems were analyzed according to the different protonated states of inhibitor and enzyme (acid/base carboxyl group, Glu166). The simulations gained quite a reasonable result according to the thermodynamic experimental fact. Further conclusions were made including the following: (1) 1-deoxynojirimycin binds with the β-glucosidase as conjugate acid forms; (2) the slow onset inhibition of isofagomine aims to slow deprotonation of the acid/base carboxyl group which is caused by a nearly zero hydrogen bond interaction between the hydroxyls of the acid/base carboxyl group; and (3) the nucleophile carboxyl group plays an important role when the inhibitor binds with glucosidase.

Introduction

The inhibitors of glycosidases are subject to intense current interest for they not only serve as important tools for studying the biological functions of oligosaccharides and the hydrolysis mechanism of glycosidases but also are prospective therapeutic agents for a variety of carbohydrate-mediated diseases.[1−3] The iminosugar achieved by the ring oxygen or anomeric carbon of pyranose or furanose replaced by the imino group is a kind of most potent glycosidase inhibitor.[4−8] These unique molecules promise a new generation of iminosugar-based medicines in a wide range of diseases such as diabetes,[9] viral infections,[10] tumor metastasis,[11] and lysosomal storage disorders.[12]

Of them, 1-deoxynojirimycin **(1, Chart 1)** and isofagomine **(2,** Chart 1**)** are of particular interest in inhibitor design for they and their derivatives are often powerful inhibitors of glycosidase action.[5,6,13,14] The mechanism of inhibition is thought of as their conjugate acid mirrors positive charge development at the endocyclic oxygen or the anomeric carbon of the glycosidase transition state **(3,** Chart 1**)** so that they can gain a tight binding complex with the glycosidase enzyme.[15] Though there is little structure difference between **1** and **2**, the inhibiting properties of them toward β-glycosidase are rather dissimilar: (1) **2** is a much more stronger inhibitor than **1** for sweet almond β-glycosidase and some other β-glycosidases.[16] (2) A slow-onset inhibition is observed for **2** when binding with the enzyme, while **1** is as a linear steady-state rate.[17,18] (3) Recent van't Hoff analysis of temperature dependence of binding of **1** and racemic **2** to sweet almond β-glycosidase shows that the binding of **1** toward the enzyme was enthalpically driven, while the binding of **2** with the enzyme was with unfavorable enthalpy and was actually entropically driven.[16] This adds the odds to the inhibition mechanism that the affinity of an enzyme for a transition-state mimic should necessarily be driven by

* Corresponding author phone: 86-021-54925277; fax: 86-021-64166128; e-mail: zhoujm@mail.sioc.ac.cn (J.-M.Z.) or mbchen@mail.sioc.ac.cn (M.-B.C.).

† Chinese Academy of Sciences.

‡ East China University of Science and Technology.

10.1021/ct050168g CCC: $33.50
Published on Web 11/09/2005

Chart 1. Transition-State Analogues 1-Deoxynojirimycin (**1**), Isofagomine (**2**), and Considerable Oxocarbenium Ion Transition State (**3**) and Crystal Structure of the Inhibitor and TmGH1β-Glucosidase Complex (**4**): Protein (Cartoon), Inhibitor (CPK), Glu166 and Glu351 (Bonds), Which Was Generated by VMD Soft Package

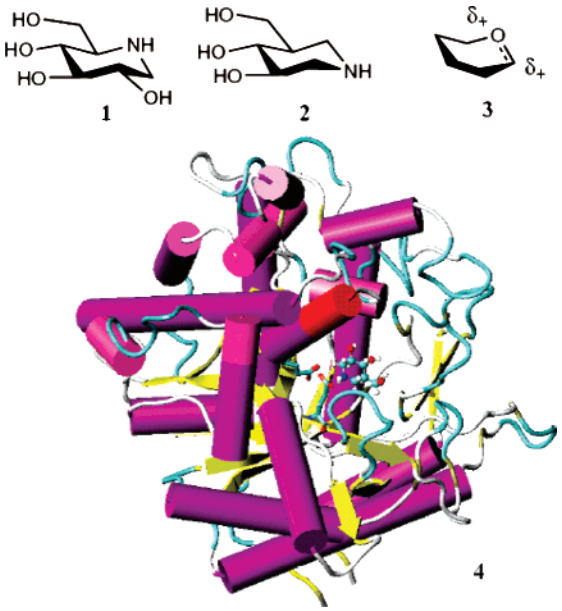

a large and favorable change in enthalpy, a criterion which was proposed by Wolfenden.[19] However, as a further study of the binding of **1** and **2** to β-glycosidase by David L. Zechel et al., in which the value of binding enthalpy was measured by the ITC (Isothermal Titration Calorimetry) method, similar favorable binding enthalpy changes were gained in contrast to the result by van't Hoff analysis, and it seems the large favorable entropy makes **2** a much better inhibitor of β-glycosidase than **1**. Otherwise, the crystal structures show that **1** binds with the TmGH1β-glycosidase in a skew-boatlike conformation while **2** is in a chair conformation, which indicates they may have different binding modes with β-glycosidase. It was suggested by the author that the superior inhibition of **2** relative to **1** is not the result of superior transition-state mimicry but benefits from an entropic advantage and a more favorable electrostatic interaction with the acid/base catalyst.[18]

The studies referred above, assuredly, gave close insight into the mechanism of inhibition. However, there are still a few questions remaining intangible. What causes an entropic advantage of **2** comparing to **1** when binding with β-glycosidase? An explanation was given that such entropic advantage may be caused by the binding of **1** incorporating approximately 1−3 more water molecules at the molecular interface relative to the binding of **2**. This has been observed in the crystal structure, but no evidence was shown in solution. **2** show a slow-onset inhibition toward the enzyme while **1** does not. The explanation of a slow conformational change in the enzyme or an unusual change of the ionization state of the inhibitor residues has been proposed, and each has some evidences. However, do they have some relationship, which means that the conformational change in the enzyme may perhaps be caused by the change of ionization

Chart 2. Label of the Glucosidase and Inhibitors: Glucosidase with Glu166 Protonated (TmGH), Glucosidase with Glu166 Unprotonated (TmG), 1-Deoxynojirimycin (DNJ), the Conjugate Acid of 1-Deoxynojirimycin (HDNJ), and the Conjugate Acid of Isofagomine (HISO)

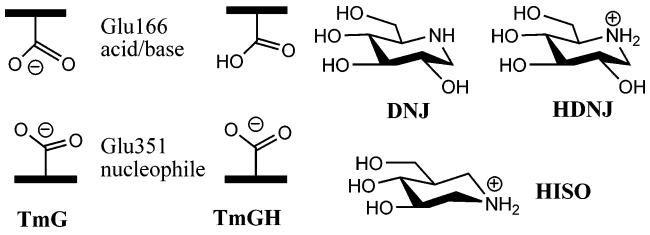

state of the inhibitor residues? Molecular dynamics in the water box can always get some useful information of the dynamic property of protein in water, and it is also an effective way to study the folding and unfolding or changes of conformation of protein in water. [20,21] Therefore, molecular dynamics will be a particularly suitable means to explore the problems which have been mentioned above.

In particular, **1** (pK_a, 6.7) would be largely unprotonated when entering the active site under pH 6−7, and it has long been argued that **1** may bind to glucosidases as a neutral amine rather than a protonated conjugate acid.[18,22,23] Additionally, as for the glucosidase, the pK_a values of the carboxyl groups of acid/base (Glu166) and nucleophile (Glu351) deduced from the pH dependence of K_{cat}/K_m are respectively 6.96 and 4.75,[18] which indicates that the nucleophile carboxyl group would be mainly unprotonated, while the acid/base carboxyl group could be both unprotonated and protonated species. So the mostly possible combined mode would be TmGH-DNJ or TmG-HDNJ. Otherwise, isofagomine (pK_a, 8.6) would be expected to be largely protonated when entering the active site at pH 6−7. Evidence from the crystal structure of the complex shows that the iminosugar is protonated within the active site, and the two carboxyl groups of acid/base and nucleophile are both unprotonated.[24] Therefore, the process of inhibitor binding with glucosidase should include deprotonation of the acid/base carboxyl group (Glu166). So in our study, the simulations TmGH-DNJ, TmG-HDNJ, TmGH-HISO, and TmG-HISO (label shown as Chart 2), summarized in Table 1, were performed.

Material and Methods

The models of TmG-HDNJ and TmGH-DNJ were built up based on the X-ray crystal of complex of **1** and TmGH1β-glycosidase at 2.2 Å resolution (PDB entry code, loim). [18] The missing residues (Ser1, Asn2, Glu233) and many other missing atoms were repaired according to the X-ray crystal structure of TmGH1β-glycosidase (PDB entry code 1od0)[18] with the molecular modeling software package Sybyl 6.9 (Tripos Inc.). The hydrogens of HDNJ and DNJ were added using the build/edit menu which is included in the Sybyl software package, and then the charge of the structures were calculated at the B3LYP/6-311++G** level using the "pop=CHelpG" keywords[25] in the Gaussion98a software package. [26] The models of TmG-HISO and TmGH-HISO were built up based on the X-ray crystal of complex of **2**

Table 1. Summary of the Molecular Dynamics Simulations

simulation label	solute (glucosidase and inhibitor)	number of water	simulation length (ns)
TmGH-DNJ	TmGH1 (Glu166 protonated), 1-deoxynojirimycin	16159	6
TmG-HDNJ	TmGH1 (Glu166 unprotonated), conjugate acid of 1-deoxynojirimycin	16159	6
TmGH-HISO	TmGH1 (Glu166 protonated), conjugate acid of Isofagomine	16788	6
TmG-HISO	TmGH1 (Glu166 unprotonated), conjugate acid of Isofagomine	16788	6

and TmGH1 β-glycosidase at 2.2 Å resolution (PDB entry code, 1oif).[18] The missing residues (Ser1, Asn2) and atoms repair of protein and the hydrogen addition of HISO as well as the charge calculation were done by the same way as models TmG-HDNJ and TmGH-DNJ. Topology files were generated using the pdb2gmx program included in the GROMACS software package and OPLS force field parameters were applied except for the charge upon the inhibitors (HDNJ, DNJ, and HISO). [27] The hydrogen atoms of the protein were also added. For TmG-HDNJ and TmG-HISO, the residue Glu166 was set unprotonated. For TmGH-DNJ and TmGH-HISO, Glu166 was set protonated. Each model was solvated with SPC water molecules in a cube box and ensured the whole surface of the protein to be covered by a water layer with a thickness more than 12 Å. Several (9 or 10) Na^+ ions were added to the system to keep it zero net charge.

The energy minimization for each model was performed using the steepest descent algorithm (100 steps), followed by the conjugate gradient (1000 steps) in the GROMACS 3.1.4 software package.[28] Then a 100 ps position restrained molecular dynamics was performed with the protein and inhibitor fixed in order to let the waters and Na^+ equilibrate around them. Finally, a 6-ns molecular dynamics was started by taking initial velocities from a Maxwellian distribution at 300 K. Solvent and solute were independently, weakly coupled to a temperature bath with a relaxation time of 0.1 ps. The system was also isotropically, weakly coupled to a pressure bath at 1.0 atm with a relaxation time of 0.5 ps and an isothermal compressibility of 0.45×10^{-4}. [29] Long-range electrostatics was calculated with the particle-mesh Ewald method. [30] Short-range van der Waals and Coulombic interactions were cut off at 1.0 and 1.0 nm, respectively. All bond lengths were constrained using the LINCS algorithm,[31] and the time step was set to 0.002 ps. When the molecular dynamics were finished, analyses were performed using facilities within the GROMACS package.

The binding free energy between the inhibitor and the enzyme was calculated using the LIE (linear interaction energy) method developed by Åqvist et al.[32,33] The LIE method is based on the assumption that, using MD or Monte Carlo conformational simulations, the binding free energy of an inhibitor to a receptor target can be expressed as the equation

$$\Delta G_{\text{bind}} = \alpha[\langle V_{\text{i-s}}^{\text{vdw}}\rangle_{\text{bound}} - \langle V_{\text{i-s}}^{\text{vdw}}\rangle_{\text{free}}] + \beta[\langle V_{\text{i-s}}^{\text{ele}}\rangle_{\text{bound}} - \langle V_{\text{i-s}}^{\text{ele}}\rangle_{\text{free}}] + \gamma$$

where $\langle\ \rangle$ denotes MD or MC averages of the nonbonded van der Waals (vdw) and electrostatic (ele) interactions between the inhibitor and its surrounding environment (i-s), i.e., either the solvated receptor binding site (bound state) or just the solvent (free state). α and β are the scaling factors for the averaged van der Waals energies and the averaged electrostatic energies. The scaling factors α β tend to be system dependent, and γ is always set to zero. For our calculation, α is set to 0.181 for all systems, and β is set to 0.33 or 0.50 when the inhibitor is a neutral amine or a protonated conjugate acid, respectively, based on Åqvist et al.'s work.[34]

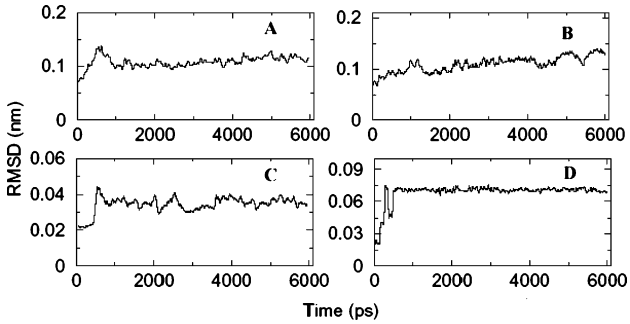

Figure 1. Time dependence of Cα RMSD of the protein with respect to the crystal structure: (A) simulation TmG-HDNJ and (B) simulation TmGH-DNJ. Time dependence of RMSD of the ligand with respect to the crystal structure: (C) simulation TmG-HDNJ and (D) simulation TmGH-DNJ. All curves are obtained by 30 ps average.

Results

The Simulations of TmG-HDNJ and TmGH-DNJ. As described above, TmGH-DNJ or TmG-HDNJ may be the most possible combined mode for **1** binding with the enzyme. Simulations TmGH-DNJ and TmG-HDNJ were performed to verify which binding mode would be mostly likely. The root-mean-square deviation of between the instantaneous MD and crystal structure was reported in Figure 1. Both simulations reach a structural equilibrium after about 1200 ps, and the RMSD values of Cα of protein are not beyond 0.15 nm, which indicates that the protein structure in solution has a small deviation from that in the crystal. As for the simulation TmG-HDNJ, the RMSD values of Cα of protein keep quite stable after it reaches a structural equilibrium while the RMSD values of HDNJ keep fluctuating around 0.04 nm, and the ring conformation of inhibitor keeps a skew-boatlike form. For simulation TmGH-DNJ, the RMSD values of Cα of protein fluctuate in a range of about 0.05 nm after 4 ns, while the RMSD values of DNJ keep fluctuating around 0.06 nm, and the ring conformation of the inhibitor stays in a chairlike form. Thus, the RMSD analysis indicates some differences between simulation TmG-HDNJ and TmGH-DNJ both in the dynamic property of protein and conformation of ligand.

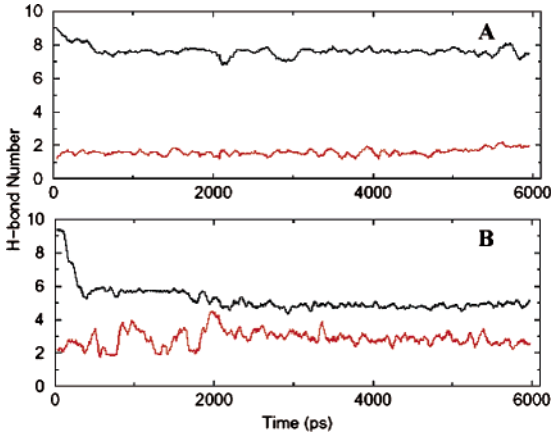

Figure 2. Time dependence of the number of hydrogen bonds: (A) simulation TmG-HDNJ, the number of hydrogen bonds between ligand and protein (black line), the number of hydrogen bonds between ligand and solvent (red line) and (B) simulation TmGH-DNJ, the number of hydrogen bonds between ligand and protein (black line), the number of hydrogen bonds between ligand and solvent (red line). All curves are obtained by 30 ps average.

The ligand has four hydroxyls and one amino (for TmGH-DNJ) or ammonium (for TmG-HDNJ) group, so the hydrogen bond interaction between the ligand and the protein as well as solvent molecules at the active site is very important for the inhibitor to bind tightly with the enzyme. Time dependence of the number of hydrogen bonds was shown in Figure 2. For simulation TmG-HDNJ, the number of hydrogen bonds between the ligand and the protein is around 8 after equilibrium, and the hydrogen bond number between the ligand and the solvent is around 2. However, for simulation TmGH-DNJ, the number of hydrogen bonds between the ligand and the protein is around 5 after equilibrium, and the number of hydrogen bonds between the ligand and the solvent is around 3. All together, the TmG-HDNJ binding mode has about two more hydrogen bonds than the TmGH-DNJ binding mode, which would cause more tightly binding between the ligand and receptor.

Snapshots of the active site structure of both simulations at 4 ns were shown in Figure 3, which can give more details about the difference of the two combined modes. As for simulation TmG-HDNJ, when the ligand is the conjugate acid of **1**, the residues Gln20, Asn165, Glu351, and Glu405 form hydrogen bonds with a ligand directly, while Glu166 forms a solvent-mediated hydrogen bond with the ligand. Of them, Glu351 is extremely important, for it forms a strong hydrogen bond with both 2-hydroxyl and ammonium of the conjugate acid. Otherwise, there are two water molecules forming a hydrogen bond with the ligand. The pyranoid ring of the ligand is distorted as a skew-boat conformation and fits the structure in crystal very well. As for simulation TmGH-DNJ, when the ligand is 1-deoxynojirimycin, His121, Glu166, Glu351, Glu405, and Trp406 form hydrogen bonds with the ligand directly and Asn165 forms a solvent-mediated hydrogen bond with the ligand, while Glu351 only forms a hydrogen bond with 2-hydroxyl and a solvent-mediated hydrogen bond with 3-hydroxyl of the ligand. There are also two hydrogen bonds between the ligand and the solvent

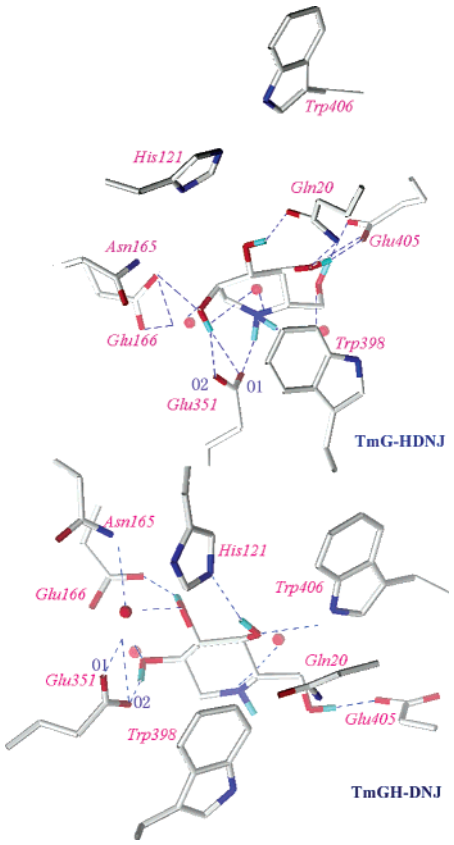

Figure 3. Snapshots of the structure of the active site of both simulations at 4 ns time step: up (simulation TmG-HDNJ) and down (simulation TmGH-HDNJ). Red balls are as water molecules.

molecule. The pyranoid ring conformation of the ligand of simulation TmGH-DNJ adopts a chairlike form rather than a skew-boat conformation for TmG-HDNJ, which does not fit that in the crystal structure.

For Glu351 plays an important role as the ligand binds with the receptor, the distances from amine or ammonium, 2-hydroxyl of the ligand to the two oxygen atoms of the carboxyl group of Glu351 were examined along all the MD simulation, and the result was reported in Figure 4. As for simulation TmG-HDNJ, the distance from O1 of the carboxyl group of Glu351 to H (N^+H_2) of the ligand is always shorter than 2.0 Å with the average of 1.6 Å; the distance from O1 of the carboxyl group of Glu351 to H (2-OH) of the ligand is between 2.0 and 3.0 Å with the average of 2.6 Å; the distance from O2 of the carboxyl group of Glu351 to H (2-OH) of the ligand fluctuates around 2.0 Å with the average of 1.9 Å. These indicate that there is a strong interaction between the residue Glu351 and the ligand and that such an interaction may contribute greatly to tightly binding of the ligand toward the receptor. As for simulation TmGH-DNJ, distances both from O1 of the carboxyl group of Glu351 to H (NH) of the ligand and from O2 of the carboxyl group of Glu351 to H (2-OH) of the ligand grow to more than 3.5 Å soon after the start of the simulation, due to the conformational change of the ligand from a skew-boatlike form to a chairlike form at about 200 ps; only the distance from O1 of the carboxyl group of Glu351 to H (2-OH) of the ligand stays below 2.0 Å and the average is 1.7 Å. Therefore,

Table 2. Average Interaction Energies (kJ/mol) between Ligand and Surroundings in the Bound and Unbound States in MD Simulation and Binding Free Energy Calculated by LIE (Linear Interaction Energy) Method Comparing with Observed Binding Free Energy Value

binding mode	$\langle V_{i-s}^{vdw}\rangle_{free}$	$\langle V_{i-s}^{vdw}\rangle_{bound}$	$\langle V_{i-s}^{el}\rangle_{free}$	$\langle V_{i-s}^{el}\rangle_{bound}$	ΔG_{bind}	observed ΔG_{bind}
TmGH-DNJ	-15.48 ± 1.22	-49.59 ± 3.38	-245.83 ± 2.81	-236.68 ± 0.36	-3.15 ± 2.42	-33.30 ± 0.00
TmG-HDNJ	-5.13 ± 0.12	-33.04 ± 1.79	-282.48 ± 0.42	-365.88 ± 4.43	-46.75 ± 2.77	

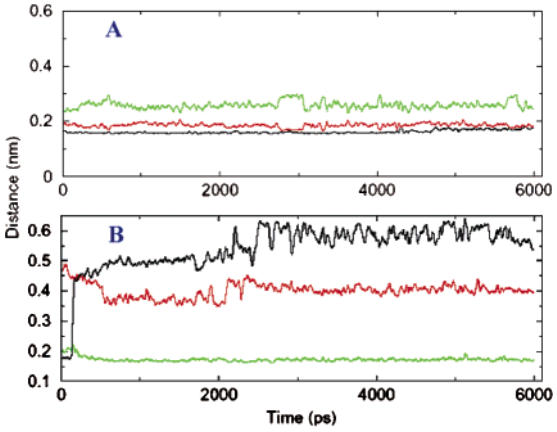

Figure 4. Time dependence of distances from amine or ammonium, 2-hydroxyl of the ligand to the two oxygen atoms of the carboxyl group of Glu351: (A) simulation TmG-HDNJ, distance from O1 of the carboxyl group of Glu351 to H (N^+H_2) of the ligand (black line), distance from O1 of the carboxyl group of Glu351 to H (2-OH) of the ligand (green line), distance from O2 of the carboxyl group of Glu351 to H (2-OH) of the ligand (red line) and (B) simulation TmGH-DNJ, distance from O1 of the carboxyl group of Glu351 to H (NH) of the ligand (black line), distance from O1 of the carboxyl group of Glu351 to H (2-OH) of the ligand (green line), distance from O2 of the carboxyl group of Glu351 to H (2-OH) of the ligand (red line). The atom label O1, O2 was shown as in Figure 3. All curves are obtained by 30 ps average.

Glu351 would contribute much less to the binding of the ligand toward the receptor when the ligand is the free amine rather than the conjugate acid.

The binding free energy was calculated using the LIE method for both binding modes TmG-HDNJ and TmGH-DNJ, respectively. Default scaling factors $\alpha = 0.181$ and $\beta = 0.50$ were used for TmG-HDNJ. For TmGH-DNJ, when the ligand is neutral, the value of β was set to 0.33. Shown in Table 2, the calculated binding free energies of the conjugate acid and the free amine are -46.75 and -3.15 kJ/mol, respectively. The observed binding energy is -33.30 kJ/mol,[18] which indicates that the conjugate acid should be the most possible state when 1-deoxynojirimycin binds with the β-glucosidase.

The Simulations of TmG-HISO and TmGH-HISO. The RMSD of both the protein and the ligand of simulation TmG-HISO and TmGH-HISO was reported in Figure 5. Also, both simulations reach a structural equilibrium after about 1200 ps. The RMSD values of Cα of the protein for both simulations stay below 0.15 nm. For simulation TmG-HISO, it is quite stable after it reaches a structural equilibrium. As for simulation TmGH-HISO, the RMSD values of Cα of the protein fluctuate between 0.1 and 0.15 nm after structural

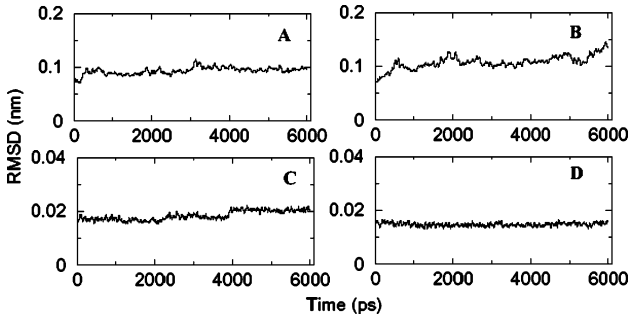

Figure 5. Time dependence of Cα RMSD of the protein with respect to the crystal structure: (A) simulation TmG-HISO and (B) simulation TmGH-HISO. Time dependence of RMSD of the ligand with respect to the crystal structure: (C) simulation TmG-HISO and (D) simulation TmGH-HISO. All curves are obtained by 30 ps average.

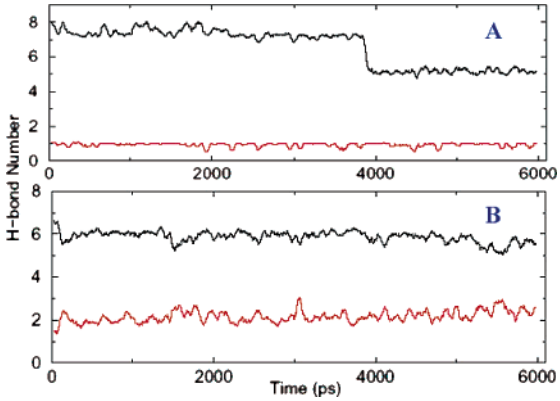

Figure 6. Time dependence of the number of hydrogen bonds: (A) simulation TmG-HISO, the number of hydrogen bonds between the ligand and the protein (black line), the number of hydrogen bonds between the ligand and the solvent (red line) and (B) simulation TmGH-HISO, the number of hydrogen bonds between the ligand and the protein (black line), the number of hydrogen bonds between the ligand and the solvent (red line). All curves are obtained by 30 ps average.

equilibrium. The RMSD values of the ligand of both simulations keep stable about 0.02 nm after equilibrium, consisting of the likewise chair $^1C_4$ conformations of the ligand in both simulations.

Time dependence of the number of hydrogen bonds was shown in Figure 6. For simulation TmG-HISO, the number of hydrogen bonds between the ligand and the protein is around 7 after equilibrium and then drops to 5 after about 4 ns, and the hydrogen bond number between the ligand and solvent is around 1. However, for simulation TmGH-HISO, the number of hydrogen bonds between the ligand and the protein is around 6 after equilibrium, and the number of

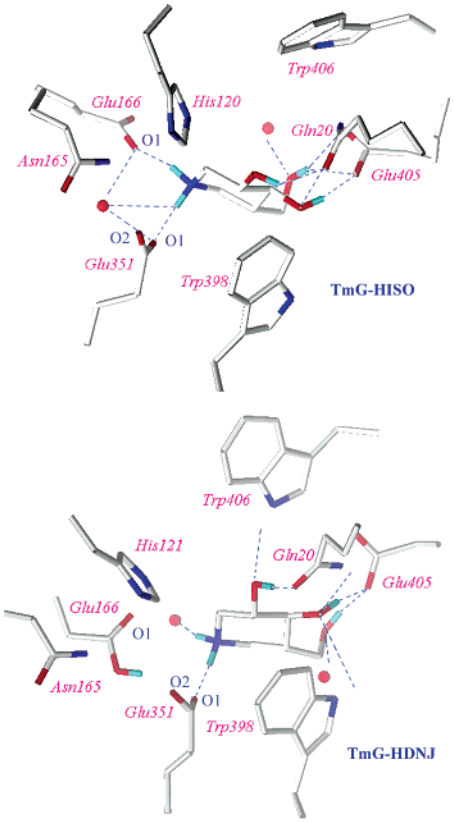

Figure 7. Snapshots of the structure of the active site of both simulations at 4 ns time step: up (simulation TmG-HISO) and down (simulation TmGH-HISO). Red balls are as water molecules.

hydrogen bonds between the ligand and the solvent is around 2. Snapshots of the active site structure of both simulations at 4 ns shown in Figure 7 provide more detailed information of the interaction between the ligand and the receptor. As for simulation TmG-HISO, when the residue Glu166 of the protein is unprotonated, the residues Gln20, Glu166, Glu351, and Glu405 form hydrogen bonds with the ligand directly, and both Glu166 and Glu351 form an additional water-mediated hydrogen bond with ligand. As for simulation TmGH-HISO, when the residue Glu166 of the protein is protonated, the residues Gln20, Glu351, Trp398, Glu405, and Glu406 form hydrogen bonds with the ligand directly, and no water-mediated hydrogen bond is found.

Residues Glu166 and Glu351 are very important for the ligand to bind tightly with the glucosidase for not only hydrogen bond interaction but also for strong electrostatic interaction between them. So the distances between the residue Glu351, Glu166, and the ligand were examined and reported in Figure 8. As for simulation TmG-HISO, distance from O1 of carboxyl group of Glu351 to H (N^+H_2) of ligand is always shorter than 2.0 Å and the average is 1.6 Å; distance from O2 of carboxyl group of Glu351 to H (N^+H_2) of ligand is always shorter than 2.0 Å and the average is 1.7 Å; distance from O1 of Glu166 to H (N^+H_2) of ligand fluctuates between 2.0 and 3.0 Å due to the rotation of torsion, then keep stable about 1.7 Å after around 2 ns. While, as for simulation TmGH-HISO, distance from O1 of carboxyl group of Glu351 to H (N^+H_2) of ligand is always shorter

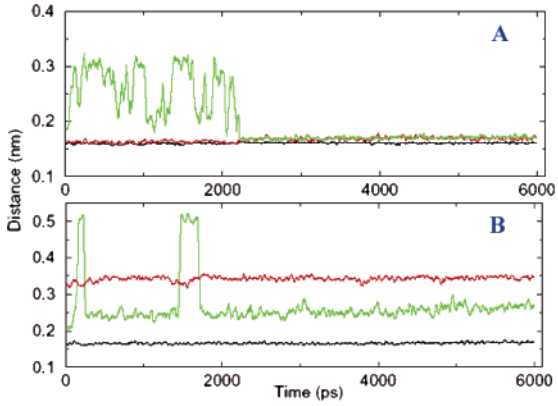

Figure 8. Time dependence of distances from ammonium of the ligand to the oxygen atoms of the carboxyl group of Glu351 and Glu166: (A) simulation TmG-HISO, distance from O1 of the carboxyl group of Glu351 to H (N^+H_2) of the ligand (black line), distance from O2 of the carboxyl group of Glu351 to H (N^+H_2) of the ligand (red line), distance from O1 of the carboxyl group of Glu166 to H (N^+H_2) of the ligand (green line) and (B) simulation TmGH-HISO, distance from O1 of carboxyl group of Glu351 to H (N^+H_2) of ligand (black line), distance from O2 of the carboxyl group of Glu351 to H (N^+H_2) of the ligand (red line), distance from O1 of the carboxyl group of Glu166 to H (N^+H_2) of the ligand (green line);

than 2.0 Å and the average is 1.7 Å; distance from O2 of carboxyl group of Glu351 to H (N^+H_2) of ligand fluctuates around 3.5 Å; distance from O1 of Glu166 to H (N^+H_2) of ligand fluctuates slightly around 2.5 Å except for two steep leap to 5.0 Å. From the result of distance analysis, we can see, when the Glu166 is unprotonated, the interaction between Glu166, Glu351, and the ligand would be much stronger than that when Glu166 is protonated, and this would compensate inferior position taken by the less number of hydrogen bond interaction. Results of binding free energy calculation were reported in Table 3. When the Glu166 of glucosidase is unprotonated, the binding free energy of ligand toward glucosidase is −41.87 kJ/mol, which is quite reasonable in contrast to the observed binding free energy − 45.60 kJ/mol. When the Glu166 of glucosidase is protonated, the binding free energy of ligand is −38.51 kJ/mol. As a comparison, the TmG-HISO binding mode is about 3.4 kJ/mol favored in contrast to the TmGH-HISO binding mode.

Discussion

The Binding Mode of 1-Deoxynojirimycin with β-Glucosidase. Though much of the published work assumes 1-deoxynojirimycin binds with glucosidase as the protonated form, which mimics the positive charge development at the anomeric carbons of the glycosidase transition state,[4,15] it has long been argued that 1-deoxynojirimycin may bind to glucosidases as a neutral amine rather than a protonated conjugate acid.[18,22,23] As the result of simulation TmG-HDNJ and TmGH-DNJ, we found that the MD snapshot structure fit better with the crystal structure when the ligand is a conjugate acid than when the ligand is a neutral amine. Furthermore, the binding free energy calculated by the LIE method indicates that the protonated ligand binds more tightly than the neutral ligand, and also a value of −46.76 kJ/mol

Table 3. Average Interaction Energies (kJ/mol) between Ligand and Surroundings in the Bound and Unbound States in MD Simulation and Binding Free Energy Calculated by LIE (Linear Interaction Energy) Method Comparing with Observed Binding Free energy value

binding mode	$\langle V_{l-s}^{vdw}\rangle_{free}$	$\langle V_{l-s}^{vdw}\rangle_{bound}$	$\langle V_{l-s}^{el}\rangle_{free}$	$\langle V_{l-s}^{el}\rangle_{bound}$	ΔG_{bind}	observed ΔG_{bind}
TmG-HISO	-6.77 ± 0.31	-38.14 ± 0.06	-251.83 ± 1.41	-324.21 ± 0.14	-41.86 ± 0.84	-45.60 ± 1.09
TmGH-HISO	-6.77 ± 0.31	-30.60 ± 0.45	-251.83 ± 1.41	-320.23 ± 0.81	-38.52 ± 1.25	

is more reasonable than that of the neutral ligand −3.15 kJ/mol in contrast to the observed binding free energy −33.30 kJ/mol. Both evidences indicate that 1-deoxynojirimycin may bind to glucosidases as protonated conjugate acid. A 6-ns molecular dynamic in water of 1-deoxynojirimycin was also performed, and the result shows that the equilibrium conformation of the ligand in water is in the chair form. Quantum calculation results also indicate that the chair conformation seems to be more stable than the boat conformation,[35] and the relative energy is about more than 20 kJ/mol. So in the bound state, when the interaction between the neutral amine of **1** and the protein is weak, the conformation of it would tend to be in the chair form, as a result of simulation TmGH-DNJ.

The Mechanism of Slow-Onset Inhibition of Isofagomine. It was proposed that slow-onset inhibition may be consistent with a slow conformational change in the enzyme or an unusual change of the ionization state of the catalytic residues. Some evidence has been shown that the protonation state of an iminosugar which is derived from **2** has been observed in the high-resolution structure of Cel5A β-glycosidase in the complex with the inhibitor.[23] Otherwise, based on fluorescence, it was suggested that the slow-onset inhibition of almond β-glycosidase may arise from a conformational change in the enzyme that leads to a high affinity complex.[24] As a result of our simulation, glucosidase occurs little conformational change when the acid/base carboxyl group is protonated in contrast to that when the acid/base carboxyl group is unprotonated, which is based on RMSD analysis. On the other hand, the hydrogen bond interaction between the hydroxyl of the carboxyl group and water plays an important role in the dissociation of the proton in aqueous solution,[36−38] so the hydrogen bond interaction between the acid/base carboxyl group (Glu166) and the solvent was examined and was reported in Figure 9. The number of the hydrogen bond between them is nearly zero. This is perhaps caused by the strong hydrogen bond interaction between the protonated ligand and surrounding water molecules which draws water molecules away from the acid/base carboxyl group. Therefore, the deprotonation of the acid/base carboxyl group would be rather slow. What is more, there are two or three water molecules forming a hydrogen bond with the ligand when the acid/base carboxyl group is protonated, while only a single hydrogen bond is found when the acid/base carboxyl group is unprotonated. This also indicates that the deprotonation may accompany the rearrangement of water. So the deprotonation, accompanying the rearrangement of water should be a slow-onset process and is the cause of slow-onset inhibition of **2** toward the glucosidase. The process of inhibitor binding with glucosidase should probably include two stages. First the conjugate acid of isofagomine binds with the glycosidase when the carboxyl group of acid/base is protonated; afterward the acid/base group occurs deprotonation to achieve more tightly binding, and the later step would be responsible for the observed slow onset of inhibition.

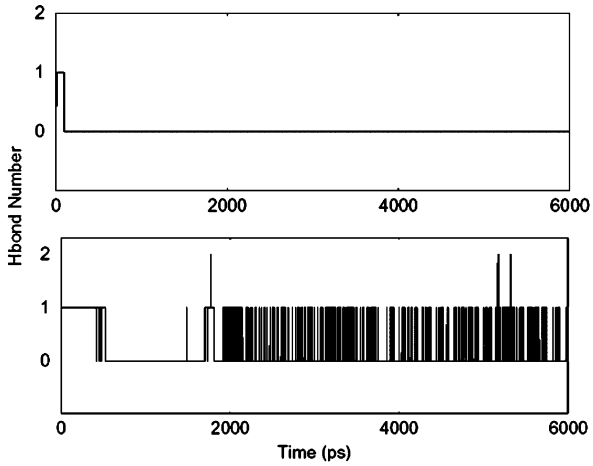

Figure 9. Time dependence of the number of hydrogen bonds between the acid/base carboxyl group (Glu166) and solvent: simulation TmGH-HISO (up) and simulation TmGH-DNJ (down) as comparison.

Thermodynamics of the Binding of Isofagomine and 1-Deoxynojirimycin. It was reported that the binding of both **2** and **1** to β-glucosidase is driven by a large and favorable enthalpy, and the large favorable entropy term makes **2** a better inhibitor than **1**.[18] As shown from the results of our simulation, the large and favorable enthalpy of both binding owes to the strong hydrogen bond and electrostatic interaction between the inhibitor and enzyme, and there is one proton release for both inhibitors when they bind with the enzyme, which is consistent with the result by quantitative analysis of the dependence of ΔH_a on the heat of ionization of the buffer. [18] Shown as hydrogen analysis (Figure 6.A), **2** coordinates only one water molecule which may contribute to the large favorable entropy, while **1** coordinates more than two water molecules (Figure 2.A) together with conformational distortion and may result in an unfavorable entropy. Furthermore, at least one more incorporated water molecule was observed for the binding of **1** with the enzyme relative to that of **2**, which is a reasonable explanation for about nearly −292 J/mol relative difference of heat capacity ($\Delta\Delta C_p$) between the binding of **1** and the binding of **2**.[18,39] The conformation of inhibitor would be largely determined by the interaction between the carboxyl group of the nucleophile and the inhibitor. Shown in Figure 10, as the ligand is 1-deoxynojirimycin, both the imino group and the 2-OH form a strong interaction with the nucleophile carboxyl group, and the ring of the inhibitor is distorted in a skew-boatlike form. While for isofagomine, only the imino group

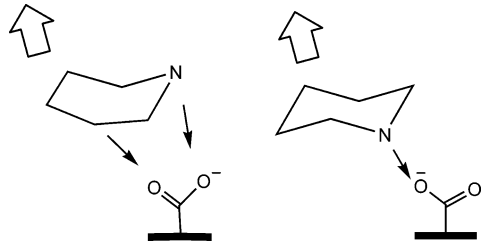

Figure 10. The illumination of the ring conformational of inhibitor induced by the nucleophile carboxyl group: when the inhibitor is 1-deoxynojirimycin (left), when the inhibitor is isofagomine (right), the interaction between the ligand and the nucleophile carboxyl group (black arrow), and the other interaction between ligand and enzyme (white arrow).

forms a strong interaction with the nucleophile carboxyl group, which results in a chairlike form.

Conclusion

1-Deoxynojirimycin and isofagomine are the representations of two sorts of imino-sugar inhibitors which are achieved by the ring oxygen or anomeric carbon of pyranose replaced by the imino group, respectively. These two inhibitors have a distinct thermodynamics property when they bind with β-glucosidase. Nanosecond time scale MD simulations of their complex with β-glucosidase were performed to examine these, and the result is quite reasonable in contrast to the experimental fact. What is more, several interesting conclusions were made and shown as follows:

(1) Just as isofagomine, 1-deoxynojirimycin may bind with the β-glucosidase as a conjugate acid forms according to the comparison of calculated binding free energy and observed binding free energy as well as the comparison of MD snapshot structure and crystal structure.

(2) The slow onset inhibition of isofagomine owns to slow deprotonation of the acid/base carboxyl group (Glu166) and combines with the rearrangement of water in the active site. The nearly zero hydrogen bond interaction between the hydroxyl of the acid/base carboxyl group would be the main cause of slow deprotonation.

(3) The nucleophile carboxyl group (Glu351) plays an important role when the inhibitor binds with glucosidase for it can form a strong hydrogen bond and an electrostatic interaction with both isofagomine and 1-deoxynojirimycin, and such an interaction may determine the ring conformation of the inhibitor.

Acknowledgment. This investigation received financial support from the Innovation Project Foundation of SIOC (Shanghai Institute of Organic Chemistry), and we also thank Dr. Ruo-Wen Wang for his constructive suggest

Supporting Information Available: The atomic charge of the structure HDNJ, DNJ, and HISO as well as the topology and force field parameter file of HDNJ, DNJ, and HISO. This material is available free of charge via the Internet at http://pubs.acs.org.

References

(1) Heightman, T. D.; Vasella, A. T. Recent insights into inhibition, structure, and mechanism of configuration-retaining glycosidase. *Angew. Chem., Int. Ed. Engl.* **1999**, *38*, 750−770.

(2) Zechel, D. L.; Withers, S. G. Glycosidase mechanisms: anatomy of a finely tuned catalyst. *Acc. Chem. Res.* **2000**, *33*, 11−18.

(3) Lillelund, V. H.; Jensen, H. H.; Liang, X.; Bols, M. Recent developments of transition-state analogue glycosidase inhibitors of non-natural product origin. *Chem. Rev.* **2002**, *102*, 515−553.

(4) Kajimoto, T.; Liu, K. K.-C.; Pederson, R. L.; Zhong, Z.; Ichikawa, Y.; Porco, J. A., Jr.; Wong, C.-H. Enzyme-catalyzed aldol condensation for asymmetric synthesis of azasugars: synthesis, evaluation, and modeling of glycosidase inhibitors. *J. Am. Chem. Soc.* **1991**, *113*, 6187−6196.

(5) Dong, W.; Jespersen, T.; Bols, M.; Skrydstrup, T.; Sierks, M. R. Evaluation of isofagomine and its derivatives as potent glycosidase inhibitor. *Biochemistry* **1996**, *35*, 2788−2795.

(6) Ichikawa, Y.; Igarashi, Y.; Ichikawa, M.; Suhara, Y. 1-*N*-Iminosugars: potent and selective inhibitors of β-Glycosidases. *J. Am. Chem. Soc.* **1998**, *120*, 3007−3018.

(7) Kim, Y. J.; Ichikawa, M.; Ichikawa, Y. A rationally designed inhibitor of α-1,3-galactosyltransferase. *J. Am. Chem. Soc.* **1999**, *121*, 5829−5830.

(8) Tanaka, K. S. E.; Winters, G. C.; Batchelor, R. J.; Einstein, F. W. B.; Bennet, A. J. A new structural motif for the design of potent glucosidase inhibitors. *J. Am. Chem. Soc.* **2001**, *123*, 998−999.

(9) Andersen, B.; Rassov, A.; Westergaard, N.; Lundgren, K. Inhibition of glycogenolysis in primary rat hepatocytes by 1,4-dideoxy-1,4-imino-d-arabinitol. *Biochem. J.* **1999**, *342*, 545−550.

(10) Durantel, D.; Branza-Nichita, N.; Carrouee-Durantel, S.; Butters, T. D.; Dwek, R. A.; Zitzmann, N. Study of the mechanism of antiviral action of iminosugar derivatives against bovine viral diarrhea virus. *J. Virol.* **2001**, *75*, 8987−8998.

(11) Goss, P. E.; Baker, M. A.; Carver, J. P.; Dennis, J. W. Inhibitors of carbohydrate processing: A new class of anticancer agents. *Clin. Cancer Res.* **1995**, *1*, 935−944.

(12) Sawkar, A. R.; Cheng, W.-C.; Beutler, E.; Wong, C.-H.; Balch, W. E.; Kelly, J. W. Chemical chaperones increase the cellular activity of N370S beta-glucosidase: A therapeutic strategy for Gaucher disease. *Proc. Natl. Acad. Sci. U.S.A.* **2002**, *99*, 15428−15433.

(13) Tan, A.; van den Broek, L.; van Boeckel, S.; Ploegh, H.; Bolscher, J. Chemical modification of glucosidase inhibitor 1-Deoxynojirimycin. *J. Biol. Chem.* **1991**, *266*, 14504−14510.

(14) Hempel, A.; Camerman, N.; Mastropaolo, D.; Camerman, A. Glucosidase inhibitor: Structure of deoxynojirimycin and castanospermine. *J. Med. Chem.* **1993**, *36*, 4082−4086.

(15) Bols, M. 1-Aza Sugars, Apparent Transition State Analogues of Equatorial Glycoside Formation/Cleavage. *Acc. Chem. Res.* **1998**, *31*, 1−8.

(16) Bülow, A.; Plesner, I. W.; Bols, M. A Large difference in the thermodynamics of binding of isofagomine and 1-deoxynojirimycin to β-glucosidase. *J. Am. Chem. Soc.* **2000**, *122*, 8567−8568.

(17) Lohse, A.; Hardlei, T.; Jensen, A.; Plesner, I. W.; Bols, M. Investigation of the slow inhibition of almond β-glucosidase and yeast isomaltase by 1-azasugar inhibitors: evidence for the 'direct binding' model. *Biochem. J.* **2000**, *349*, 211−215.

(18) Zechel, D. L.; Boraston, A. B.; Gloster, T.; Boraston, C. M.; Macdonald, J. M.; Tilbrook, D. M. G.; Stick, R. V.; Davies, G. J. Iminosugar Glycosidase Inhibitors: Structural and Thermodynamic Dissection of the Binding of Isofagomine and 1-Deoxynojirimycin to β-Glucosidases. *J. Am. Chem. Soc.* **2003**, *125*, 14313−14323.

(19) Wolfenden, R.; Snider, M. J. The depth of chemical time and the power of enzymes as catalysts. *Acc. Chem. Res.* **2001**, *34*, 938−945.

(20) Karplus, M.; McCammon, J. A. Molecular dynamics simulations of biomolecules. *Nature Struct. Biol*. **2002**, *9* (9), 646−652.

(21) Cardona, F.; Goti, A.; Brandi, A.; Scarselli, M.; Niccolai, N.; Mangani, S. Molecular dynamics simulations on the complexes of glucoamylase II (471) from *Aspergillus awamori* var. X100 with 1-deoxynojirimycin and lentiginosine. *J. Mol. Model.* **1997**, *3*, 249−260.

(22) Dale, M. P.; Ensley, H. E.; Kern, K.; Sastry, K. A.; Byers, L. D. Reversible inhibitors if β-glucosidase. *Biochemistry* **1985**, *24*, 3530−3539.

(23) Legler, G. Glycoside hydrolases: mechanistic information from studies with reversible and irreversible inhibitors. *Adv. Carbohydr. Chem. Biochem.* **1990**, *48*, 319−385.

(24) Varrot, A.; Tarling, C. A.; Macdonald, J. M.; Stick, R. V.; Zechel, D. L.; Withers, S. G.; Davies, G. J. Direct observation of the protonation state of an imino sugar glycosidase inhibitor upon binding. *J. Am. Chem. Soc.* **2003**, *125*, 7496−7497.

(25) Breneman, C. M.; Wiberg, K. B. Determining Atom-Centered Monopoles from Molecular Electrostatic Potentials. The Need for High Sampling Density in formamide Conformational Analysis. *J. Comput. Chem.* **1990**, *11*, 361−373.

(26) Frisch, M. J.; Trucks, G. W.; Schlegel, H. B.; Scuseria, G. E.; Robb, M. A.; Cheeseman, J. R.; Zakrzewski, V. G.; Montgomery, J. A., Jr.; Stratmann, R. E.; Burant, J. C.; Dapprich, S.; Millam, J. M.; Daniels, A. D.; Kudin, K. N.; Strain, M. C.; Farkas, O.; Tomasi, J.; Barone, V.; Cossi, M.; Cammi, R.; Mennucci, B.; Pomelli, C.; Adamo, C.; Clifford, S.; Ochterski, J.; Petersson, G. A.; Ayala, P. Y.; Cui, Q.; Morokuma, K.; Malick, D. K.; Rabuck, A. D.; Raghavachari, K.; Foresman, J. B.; Cioslowski, J.; Ortiz, J. V.; Stefanov, B. B.; Liu, G.; Liashenko, A.; Piskorz, P.; Komaromi, I.; Gomperts, R.; Martin, R. L.; Fox, D. J.; Keith, T.; Al-Laham, M. A.; Peng, C. Y.; Nanayakkara, A.; Gonzalez, C.; Challacombe, M.; Gill, P. M. W.; Johnson, B. G.; Chen, W.; Wong, M. W.; Andres, J. L.; Head-Gordon, M.; Replogle, E. S.; Pople, J. A. *Gaussian 98*, revision A.9; Gaussian, Inc.: Pittsburgh, PA, 1998.

(27) (a) Jorgensen, W. L.; Maxwell, D. S.; Tirado-Rives, J. *J. Am. Chem. Soc.* **1996**, *118*, 11225−11236. (b) Jorgensen, W. L.; McDonald, N. A. *Theochem.* **1998**, *424*, 145−155. (c) Jorgensen, W. L.; McDonald, N. A. *J. Phys. Chem. B* **1998**, *102*, 8049−8059. (d) Rizzo, R. C.; Jorgensen, W. L. *J. Am. Chem. Soc.* **1999**, *121*, 4827−4836. (e) Watkins, E. K.; Jorgensen, W. L. *J. Phys. Chem. A.* **2001**, **105**, 4118−4125.

(28) (a) Berendsen, H. J. C.; van der Spoel, D.; van Drunen, R. GROMACS: A message-passing parallel molecular dynamics implementation. *Comput. Phys. Comm.* **1995**, *91*, 43−56. (b) Lindahl, E.; Hess, B.; van der Spoel, D. GROMACS 3.0: A package for molecular simulation and trajectory analysis *J. Mol. Model.* **2001**, *7*, 306−317.

(29) Berendsen, H. J. C.; Postma, J. P. M.; DiNola, A.; Haak, J. R. Molecular dynamics with coupling to an external bath. *J. Chem. Phys.* **1984**, *81*, 3684−3690.

(30) Essmann, U.; Perera, L.; Berkowitz, M. L.; Darden, T.; Lee, H.; Pedersen, L. G. A smooth particle mesh Ewald potential. *J. Chem. Phys.* **1995**, *103*, 8577−8592.

(31) Hess, B.; Bekker, H.; Berendsen, H. J. C.; Fraaije, J. G. E. M. LINCS: A linear constraint solver for molecular simulations. *J. Comput. Chem.* **1997**, *18*, 1463−1472.

(32) Åqvist, J.; Luzhkov, V. B.; Brandsdal, B. O. Ligand binding affinities from MD simulations. *Acc. Chem. Res.* **2002**, *35*, 358−365.

(33) Marelius, J.; Graffner-Nordberg, M.; Hansson, T.; Hallberg, A.; Åqvist, J. Computation of affinity and selectivity: Binding of 2,4-diaminopteridine and 2,4-diaminoquinazoline inhibitors to dihydrofolate reductases. *J. Comput.-Aided Mol. Des.* **1998**, *12*, 119−131.

(34) Hansson, T.; Marelius, J.; Åqvist, J. Ligand Binding Affinity, Prediction by Linear Interaction Energy Methods. *J. Comput.-Aided Mol. Des.* **1998**, *12*, 27−35.

(35) (a) Single-point energies were calculated at the B3LYP/6-311++G(2d, 2p) level. The free energies of solvation in water ΔG_s° were calculated utilizing the AM1-SM5.4 solvation model. (b) Hawkins, G. D.; Giesen, D. J.; Lynch, G. C.; Chambers, C. C.; Rossi, I. J. AMSOL-version 6.8.

(36) Chipot, C.; Gorb, L. C.; Rivail, J.-L. Proton Transfer in the Mono- and the Dihydrated Complexes of HF and HCl: An MP2/6-31+G** ab Initio Study in the Self-Consistent Reaction Field Model of Solvation. *J. Phys. Chem.* **1994**, *98*, 1601−1607.

(37) Smith, A.; Vincent, M. A.; Hillier, I. H. Mechanism of acid dissociation in water clusters: Electronic structure studies of $(H_2O)_nHX$ ($n = 4, 7$; X = OH, F, HS, HSO_3, $OOSO_2H$, $OOH{\cdot}SO_2$). *J. Phys. Chem. A* **1999**, *103*, 1132−1139.

(38) Voegele, A. F.; Klaus, R.; Liedl, K. R. Exploring HBr ionization at the molecular level. *Angew. Chem., Int. Ed.* **2003**, *42*, 2114−2116.

(39) Habermann, S. M.; Murphy, K. P. Energetics of hydrogen bonding in proteins: A model compound study. *Protein Sci.* **1996**, *5*, 1229−1239.

CT050168G